J Chin Med Assoc

ORIGINAL ARTICLE

Multilineage differentiation potential in the infant adipose- and umbilical cord-derived mesenchymal stem cells

Hui-Kuang Huang[a–d], Kuang-Kai Hsueh[e], Yu-Ting Liao[b,f], Szu-Hsien Wu[a,f,g], Po-Hsin Chou[b], Shih-Han Yeh[e], Jung-Pan Wang[a,b,*]

[a]Department of Surgery, School of Medicine, National Yang Ming Chiao Tung University, Taipei, Taiwan, ROC; [b]Department of Orthopaedics & Traumatology, Taipei Veterans General Hospital, Taipei, Taiwan, ROC; [c]Department of Orthopaedics, Ditmanson Medical Foundation Chiayi Christian Hospital, Chiayi, Taiwan, ROC; [d]Department of Food Nutrition, Chung Hwa University of Medical Technology, Tainan, Taiwan, ROC; [e]Department of Orthopedic Surgery, Taoyuan General Hospital, Ministry of Health and Welfare, Taoyuan, Taiwan, ROC; [f]Division of Plastic and Reconstructive Surgery, Department of Surgery, Taipei Veterans General Hospital, Taipei, Taiwan, ROC; [g]Division of Plastic and Reconstructive Surgery, Department of Surgery, School of Medicine, National Defense Medical Center, Taipei, Taiwan, ROC

Abstract

Background: This study aims to compare the biological properties of infant adipose-derived mesenchymal stem cells (infant ADSCs) from excised polydactyly fat tissue and umbilical cord-derived mesenchymal stem cells (UCSCs) in terms of proliferation and differentiation capabilities. The proliferation of infant ADSCs and UCSCs was analyzed by determining the fold changes of cell numbers and doubling time periods.

Methods: The state of senescence and replicative stress was compared by analyzing the expression of age-related genes, senescence-associated β-galactosidase (SA-β-gal) staining, and phosphorylated histone variant H2AX (γH2AX) immunofluorescence staining. The expression levels of superoxide dismutase (*SODs*) and genes related to multilineage differentiation were analyzed using reverse transcription-quantitative polymerase chain reaction (RT-qPCR). Differentiation levels were determined using histochemical staining, immunohistochemical staining, and immunofluorescence staining.

Results: Infant ADSCs exhibited higher proliferation rates and expression levels of *SOD1*, *SOD2*, and *SOD3* at passages 3–5 compared with UCSCs. Senescence related genes (*p16*, *p21*, and *p53*), SA-β-gal staining, and replicative stress analysis were reduced in infant ADSCs. The expression levels of chondrogenic genes (*COL2* and *COL10*), osteogenic genes (*RUNX2* and *ALP*), adipogenic genes (*LPL*), and hepatogenic genes (*ALB* and *TAT*) in infant ADSC-differentiated cells were significantly higher than those in UCSCs. Histochemical and immunofluorescence staining confirmed these results. Only the expression levels of tenogenic genes (*MMP3*, *DCN*, and *COL3*) in infant ADSC-differentiated cells were lower than those in UCSCs.

Conclusion: Infant ADSCs exhibit higher proliferation rates, reduced cellular senescence and replicative stress, better antioxidative activity, and higher differentiation potential toward chondrogenic, osteogenic, adipogenic and hepatogenic lineages than UCSCs.

Keywords: Infant adipose-derived mesenchymal stem cells; Multilineage differentiation; Proliferation; Senescence; Umbilical cord-derived mesenchymal stem cells

1. INTRODUCTION

Multipotent mesenchymal stem cells (MSCs) are considered to be ideal sources of stem cells for tissue regeneration because of their high proliferation ability and potential to differentiate into multiple cell types.[1] These cells can be obtained from various sources, such as adipose tissue, bone marrow, and umbilical cords.[2] Adipose-derived mesenchymal stem cells (ADSCs) and umbilical cord-derived mesenchymal stem cells (UCSCs) are particularly attractive for tissue engineering applications, as they can be collected through less invasive methods. ADSCs, which have ability to differentiate into multiple cell lineages, can be easily obtained in large quantities through liposuction and are readily cultured.[3] UCSCs, which can be obtained from umbilical cords that are typically considered medical waste, also possess the ability to differentiate into multiple cell lineages.[4,5]

UCSCs are derived from the umbilical cord matrix surrounding the vessels and are classified as mesenchymal lineage cells.[6] These cells have a short doubling time and their collection dose not present ethical limitations.[7] Furthermore, there are no medical or legal restrictions on the use of UCSCs in various applications.[8] Previous studies have reported that UCSCs have the longest culture period, with up to nine passages (P9), compared

Address correspondence. Dr Jung-Pan Wang, Department of Orthopaedics & Traumatology, Taipei Veterans General Hospital, 201, Section 2, Shi-Pai Road, Taipei 112, Taiwan, ROC. E-mail address: jpwang801@gmail.com (J.-P. Wang).

Author contributions: Dr. Hui-Kuang Huang and Dr. Kuang-Kai Hsueh contributed equally to this work.

Conflicts of interest: The authors declare that they have no conflicts of interest related to the subject matter or materials discussed in this article.

Journal of Chinese Medical Association. (2023) 86: 1083-1095.

Received June 19, 2023; accepted July 30, 2023.

doi: 10.1097/JCMA.0000000000000990

to six passages (P6) for bone marrow-derived mesenchymal stem cells (BMSCs) and ADSCs, and also exhibit the highest proliferation capacity.[2] Although UCSCs have the potential to differentiate into multiple cell types, their differentiation tendency leans towards the osteogenic lineage.[8]

One of the issues that may affect the biological properties of MSCs is aging. Biologically aged MSCs release reactive oxygen species (ROS) that cause oxidative stress in the surrounding environment. This stress can lead to the growth arrest of senescent cells and cause neighboring cells to enter a senescent state.[9,10] Replicative senescence of MSCs can affect cell behavior and regenerative capacity.[2,11] Studies have observed an age-related decline in the number of cells and proliferative capacity of BMSCs from donors of varying ages.[12] Additionally, the proliferation, viability, and differentiation potential of MSCs from aged donors are reduced when compared to those from younger ones.[13] Cellular senescence results in ROS accumulation, upregulation of tumor suppressor genes, telomere shortening, growth arrest, morphological changes in cells, and an increase in senescence-associated β-galactosidase (SA-β-gal) expression.[14]

Infant ADSCs can be isolated from excised polydactyly fat tissue, which is often discarded as surgical waste. The prevalence of polydactyly in Taiwan was 16.57 per 10 000 births between 2005 and 2014, with males being twice as likely to be affected as females.[15–17] Both infant ADSCs and UCSCs can be obtained from surgical waste and expanded in vitro to obtain large numbers of cells for experiments. Previous studies have shown that infant ADSCs exhibit less senescence and replicative stress than adult ADSCs and have better proliferation abilities, antioxidant defense, and the potential for chondrogenic, adipogenic, and neurogenic differentiation.[18] On the other hand, UCSCs are considered to be among the youngest MSCs. In this study, three UCSC cell lines were purchased from American Type Culture Collection (ATCC), with different races and genders represented in each cell line. The aim of this study is to compare the proliferation, antioxidative ability, and differentiation potential of infant ADSCs and UCSCs.

2. METHODS

2.1. Isolation and culture of UCSCs and infant ADSCs

UCSC cell lines (ATCC PCS-500-010) were purchased from ATCC (Manassas, VA, USA), and included UCSC-1 (lot number 64310874) at passage 1, UCSC-2 (lot number 70005074) at passage 2, and UCSC-3 (lot number 70014369) at passage 2.

To isolate the infant ADSCs (n = 3), the fat tissue was extracted from excised redundant thumbs or fingers of children with polydactyly after surgical reconstruction. The cases of polydactyly were sporadic without other systemic problems. The Institutional Review Board (IRB) approved the protocol and procedure. The fat sample was incubated in 0.1% collagenase (Wako, Osaka, Japan) in Hank's balanced salt solution (HBSS; Gibco, Carlsbad, CA, USA) for digestion in a shaking water bath (37°C, 30 minutes). After digestion, the stromal vascular fraction (SVF) cells were washed with PBS three times to remove the collagenase.[18] The cells were isolated and resuspended in culture medium at a concentration of approximately $2–3 \times 10^6$ cells per 10cm^2 dish.

The cells were seeded at a density of 1×10^5 cells in a 60-cm^2 dish and cultured in the Dulbecco's Modified Eagle Media (DMEM; Gibco) with low glucose (LG-DMEM), 10% fetal bovine serum (FBS; Invitrogen, Carlsbad, CA, USA), and antibiotic-antimycotic solution (Corning Life Science, Corning, NY, USA). The culture medium was changed every 2 days, and confluent cells (at a density of approximately 1×10^6 cells in a 60-cm^2 dish) were propagated at a 1:5 split every 5 to 7 days. The cells were cultured at 37°Cand 5% CO_2.

2.2. Doubling time quantification

The UCSCs and infant ADSCs were cultured in DMEM containing 10% FBS, 100 U/mL penicillin (Invitrogen), 100 μg/mL streptomycin (Invitrogen), and 250 ng/mL amphotericin B (Invitrogen). The culture medium was changed every 3–4 days.[18,19]

To calculate the population doubling time, the cells were seeded at a density of $1–2 \times 10^5$ cells in a 10-cm dish, recovered, and passaged every 7 days. The cell numbers at each passage were counted to determine the fold changes in cell numbers. This process was carried out in triplicate culture.[20]

2.3. Quantitative reverse transcription polymerase chain reaction analysis

Cellular RNA was extracted using Trizol reagent (Invitrogen). Random sequence primers and the iScript cDNA Synthesis Kit (Bio-Rad, Hercules, CA, USA) were used to synthesize the first strand complement DNA (cDNA). Real-time polymerase chain reaction (PCR) was performed to amplify the cDNA in a reaction mixture containing specific primer pairs (listed in the Table 1) and the fast SYBR Green 189 Master Mix (Applied Biosystems, Foster City, CA, USA). Glyceraldehyde-3-phosphate dehydrogenase (*GAPDH*) was used as an internal control. Analysis of the results was carried out using the software supplied with the StepOne (Applied Biosystems), and the comparative CT (ΔΔCT) method.[20]

2.4. SA-β-gal assays

To evaluate the cell senescence, a senescence β-galactosidase cell staining kit (Cell Signaling Technology, Danvers, MA, USA) was used to assay the UCSCs and infant ADSCs. Cells at passages 6–7 were seeded at a density of 1×10^5 cells per 6-cm dish and cultured for 5 days at 37°Cand 5% CO_2. The senescent cells were detected by staining in blue following the manufacturer's instructions. The stained cells were observed under a microscope.

2.5. Phosphorylated histone variant H2AX immunostaining

To perform phosphorylated histone variant H2AX (γH2AX) immunostaining, UCSCs and infant ADSCs at passage 3 were permeabilized with a permeabilization buffer (0.1% Triton X-100 in PBS) and fixed with 4% paraformaldehyde. The cells were then stained with primary antibodies (tcba13051; Taiclone Biotech Corp., Taipei, Taiwan) against the phosphorylation of the histone variant, γH2AX, at an appropriate dilution. The DyLight 488-conjugated goat anti-rabbit IgG secondary antibodies (GTX213110-01; GeneTex Inc., Irvine, CA, USA) were used to show green fluorescence. The nuclei were counterstained with 4′,6-diamidino-2-phenylindole (DAPI; F6057; Sigma-Aldrich, St Louis, MO, USA). Fluorescence intensity was determined by analyzing 60 to 100 cells using Image-Pro Plus (v4.5.0.29; Media Cybernetics, Silver Spring, MD, USA). The intensity values were normalized with the cell numbers and reported in arbitrary units.

2.6. Chondrogenic differentiation

To induce chondrogenic differentiation, UCSCs or infant ADSCs at passages 3 to 5 were cultured in a chondrogenic differentiation medium (CIM), consisting of serum-free and high-glucose (4.5 g/L) DMEM (HG-DMEM) (Gibco) supplemented with 50 mg/mL insulin-transferrin-selenium (ITS) plus Premix (BD Biosciences, San Jose, CA, USA), 10^{-7} M dexamethasone (Sigma-Aldrich), 50 mg/mL ascobate-2-phosphate (Sigma-Aldrich), and 10 ng/mL TGF-β1 (R&D Systems, Minneapolis, MN, USA). The

Table 1

Primers used for RT-qPCR analysis

Gene	Forward primer (5′-3′)	Reverse primer (5′-3′)
p16	ATCATCAGTCACCGAAGG	TCAAGAGAAGCCAGTAACC
p21	CATCTTCTGCCTTAGTCTCA	CACTCTTAGGAACCTCTCATT
p53	CGGACGATATTGAACAATGG	GGAAGGGACAGAAGATGAC
SOD1	GTGATTGGGATTGCGCAGTA	TGGTTTGAGGGTAGCAGATGAGT
SOD2	TTAACGCGCAGATCATGCA	GGTGGCGTTGAGATTGTTCA
SOD3	CATGCAATCTGCAGGGTACAA	AGAACCAAGCCGGTGATCTG
SOX9	CCAGGGCACCGGCCTCTACT	TTCCCAGTGCTGGGGGCTGT
COL2	TTCAGCTATGGAGATGACAATC	AGAGTCCTAGAGTGACTGAG
COL10	CAAGGCACCATCTCCAGGAA	AAAGGGTATTTGTGGCAGCATATT
RUNX2	ATGACGTCCCCGTCCATCCA	GGAAGGCCAGAGGCAGAAGTCA
ALP	ACCATTCCCACGTCTTCACATTTG	AGACATTCTCTCGTTCACCGCC
PPARγ	TCAGGTTTGGGCGGATGC	TCAGCGGGAAGGACTTTATGTATG
LPL	TGTAGATTCGCCCAGTTTCAGC	AAGTCAGAGCCAAAAGAAGCAGC
ALB	TGCTTGAATGTGCTGATGACAGGG	AAGGCAAGTCAGCAGGCATCTCATC
TAT	TCAGTTTCCCGTATGCCACC	ATCTTTGGGGGCTTGGATGG
MMP3	CTGTTGATTCTGCTGTTGAG	AAGTCTCCATGTTCTCTAACTG
DCN	CTCTGCTGTTGACAATGGCTCTCT	TGGATGGCTGTATCTCCCAGTACT
COL3	GGGAACATCCTCCTTCAACA	GCAGGGAACAACTTGATGGT
GADPH	ATATTGTTGCCATCAATGACC	GATGGCATGGACTGTGGTCATG

ALB = albumin; *ALP* = alkaline phosphatase; *COL2* = collagen type 2; *COL3* = collagen type 3; *COL10* = collagen type 10; *DCN* = decorin; *GAPDH* = glyceraldehyde-3-phosphate dehydrogenase; *LPL* = lipoprotein lipase; *MMP3* = matrix metallopeptidase 3; *p16* = cyclin-dependent kinase inhibitor 2A (CDKN2A); *p21* = cyclin-dependent kinase inhibitor 1A (CDKN1A); *p53* = tumor protein p53; *PPARγ* = peroxisome proliferator-activated receptor γ; *RUNX2* = runt-related transcription factor 2; *SOD1* = superoxide dismutase type 1; *SOD2* = superoxide dismutase type 2; *SOD3* = superoxide dismutase type 3; *SOX9* = SRY-box containing gene 9; *TAT* = tyrosine aminotransferase.

cells were cultured at 37°C and 5% CO_2, with the medium being changed every 3 days. On day 21 of induction, the pellets were observed and collected for further analysis.[21]

2.7. Immunohistochemistry staining of the chondrogenic pellets and quantification

The equivalent diameter of the chondrogenic pellets formed by UCSCs and infant ADSCs was measured on day 21. The pellets were embedded in paraffin, sectioned, and stained with Alcian blue (ANC500; ScyTek Laboratories, Logan, UT, USA) to detect proteoglycans. Nuclear fast red staining (NFS125; ScyTek) was used to counterstain the nuclei. To detect collagen (COL) 2 and 10, the sections were deparaffinized, hydrated, and treated with 0.4 mg/mL proteinase K for 15 minutes. Endogenous peroxidase activity was blocked with 3% hydrogen peroxide (Sigma-Aldrich). The sections were then incubated with primary antibodies against COL2 (MAB8887; Millipore Corporation, Burlington, MA, USA) or COL10 (ab58632; Abcam, Cambridge, MA, USA) overnight at 4°C. The samples were incubated with the secondary anti-rabbit polymer-horseradish peroxidase (HRP) in the Super Sensitive Polymer-HRP Detection Systems (QD420-YIKE; BioGenex, San Ramon, CA, USA) for 30 minutes. Staining was visualized with the DAB substrate and hematoxylin. The staining intensities in the areas of the infant ADSC- and UCSC-differentiated pellets were quantified using image analysis software (Image Pro Plus 4.0; Media Cybernetics, Inc., Rockville, MD, USA), and the values were compared to calculate the relative fold.

2.8. Osteogenic differentiation

The UCSCs and infant ADSCs at passages 3 to 5 were induced in an osteogenic induction medium (OIM) which was used to induce osteogenic differentiation; it was a LG-DMEM supplemented with 10% FBS, 50 μg/mL ascorbic acid-2 phosphate (Nacalai, Kyoto, Japan), 0.01 μM dexamethasone (Sigma-Aldrich), and 1 mM β-glycerol phosphate (Sigma-Aldrich) and maintained at 37°C and 5% CO_2 for 21 days.

2.9. Alizarin Red S staining

Alizarin Red S (ARS) staining is a widely used method for detecting calcium deposition in cells undergoing osteogenic differentiation. In this study, the differentiated cells were fixed and stained with ARS (A5533; Sigma-Aldrich) after 21 days of osteogenic differentiation. The stained cells were then subjected to a quantification assay to determine the extent of osteogenic differentiation. The ARS was extracted from the stained cells using a 10% cetylpyridinium chloride buffer (CPC), and the optical density (OD) of the extract was measured at 550 nm using an enzyme-linked immunosorbent assay (ELISA) reader (Spectra MAX 250; Molecular Devices, Sunnyvale, CA, USA). The OD of differentiated cells was normalized with that of undifferentiated cells, and the relative fold changes were calculated to determine the degree of osteogenic differentiation induced in the UCSCs and infant ADSCs.

2.10. Adipogenic differentiation

To induce adipogenic differentiation, UCSCs and infant ADSCs at passages 3 to 5 were treated with an adipogenic induction medium (AIM) containing LG-DMEM supplemented with 10% FBS, 50 μg/mL ascorbic acid-2 phosphate, 0.1 μM dexamethasone, 50 μM indomethacin (Sigma-Aldrich), 45 μM 3-isobutyl-1-methylxanthine (Sigma-Aldrich), and 1 μg/mL insulin (Sigma-Aldrich). The cells were incubated at 37°C and 5% CO_2 for 21 days.

2.11. Oil Red O staining

The differentiated cells were washed twice with PBS, fixed in 10% formalin for at least 1 hour at room temperature, and stained with Oil Red O (O9755; Sigma-Aldrich) for 2 hours to visualize adipogenic differentiation. The working solution of Oil Red O was prepared by mixing 15 mL of a stock solution (0.5% in isopropanol) and 10 mL of distilled water and then filtering through a polyvinylidene difluoride (PVDF) membrane (0.2 μm). Quantification of lipid accumulation was performed by extracting Oil Red O from the stained cells with isopropanol,

and the OD of the extract was measured at 510 nm using an ELISA reader (Spectra MAX 250; Molecular Devices). The OD of differentiated cells was normalized to that of undifferentiated cells, and the relative fold changes were reported.

2.12. Hepatogenic differentiation

The UCSCs and infant ADSCs were induced in a stepwise induction protocol. In step 1, cells were treated with LG-DMEM containing 20 ng/mL human epidermal growth factor (hEGF; Sigma-Aldrich) and a 10 ng/mL human fibroblast growth factor-basic (hBFGF; Sigma-Aldrich) at 37°C and 5% CO_2 for 24 hours. In step 2, the differentiation was treated with LG-DMEM supplemented with the 20 ng/mL human hepatocyte growth factor (hHGF; Sigma-Aldrich), 10 ng/mL hBFGF, and 0.61 mg/mL Nicotinamide (Sigma-Aldrich) for 7 days. In step 3, the cells were induced with LG-DMEM supplemented with 20 ng/mL Oncostatin (R&D Systems), 10^{-6} M Dexamethasone (Sigma-Aldrich), and ITS-premix (Corning Life Science) for 7 days.[22] The total process of differentiation lasted 15 days.

2.13. Immunofluorescence staining of the hepatogenic differentiated cells and quantification

On day 15, differentiated cells were fixed and stained with a primary antibody against albumin (Taiclone Biotech Corp., Taipei, Taiwan), followed by incubation with DyLight 488-conjugated goat anti-mouse IgG (A90-516D2; Bethyl Laboratories, Inc., Montgomery, TX, USA) secondary antibodies. The slides were counterstained with DAPI for nuclear staining. Immunofluorescence intensity was quantified using Image-Pro Plus v4.5.0.29.

2.14. Tenogenic differentiation

The UCSCs and infant ADSCs at passages 3 to 5 were induced in a tenogenic induction medium (TIM), containing LG-DMEM with 10% FBS, 50 μg/mL ascorbic acid (AA; Sigma Aldrich), and 100 ng/mL connective tissue growth factor (CTGF),[23] and maintained at 37°C and 5% CO_2 for 21 days.

2.15. Picrosirius red staining

Collagen deposition of the differentiated cells was evaluated using picrosirius red staining. The cells were seeded in a 24-well plate (Corning Life Science) at a density of 3×10^3 cells/cm^2, fixed in Bouin's solution (Bouin's Fixative; Electron Microscopy Sciences, Hatfield, PA, USA) for 1 hour, and stained with 0.1% picrosirius red (ScyTek Laboratories) saturated in picric acid (Sigma-Aldrich). Collagen deposition was visualized under polarized light microscopy.[24] Quantification of the stained collagen was detected by extracting the picrosirius red from the stained cells with a 0.2 M NaOH and methanol (1:1) buffer, and the OD of the extract was measured at 550 nm using an ELISA reader (Spectra MAX 250; Molecular Devices).

2.16. Statistical analysis

The quantitative data were presented as mean ± SD, and statistical analysis was performed using Prism (version 5.03; GraphPad, La Jolla, CA, USA). The Mann-Whitney *U* test was used to verify the statistical significance of the experimental results, and *p* values of less than 0.05 were considered significant.

3. RESULTS

3.1. Proliferation of the infant ADSCs and UCSCs

The morphologies and confluence of infant ADSCs and UCSCs at passages 2 and 7 were imaged (Fig. 1A). The proliferation of infant ADSCs and UCSCs from passages 2 to 8 was monitored by measuring the fold increases in the cell numbers (Fig. 1B) and the cell doubling time (Fig. 1C). The fold increases in cell numbers of infant ADSCs at passages 2 (a 33.74- ± 4.74-fold increase) and 3 (a 27.76- ± 5.04-fold increase) was significantly higher than that of UCSCs (a 7.93- ± 0.66-fold increase and a 16.66- ± 1.93-fold increase, respectively). The doubling time of infant ADSCs at passages 2 (1.1 ± 0.15 days), 7 (1.75 ± 0.10 days), and 8 (1.81 ± 0.05 days) were also significantly shorter than that of UCSCs (2.02 ± 0.08 days, 2.53 ± 0.43 days, and 2.49 ± 0.06 days, respectively). These results suggest that UCSCs require an activation period (P2–P3) to achieve their full proliferative potential, after which their proliferation declines. In contrast, the proliferation of infant ADSCs declined in every passage, indicating the culture caused rapid senescence. However, the preservation of the proliferation trend in infant ADSCs was better than that in UCSCs.

3.2. Senescence, replicative stress, and anti-oxidative ability in the infant ADSCs and UCSCs

The expression of aging-related genes, including cyclin-dependent kinase inhibitor 2A (CDKN2A, *p16*) and cyclin-dependent kinase inhibitor 1A (CDKN1A, *p21*), was significantly higher in the UCSCs at early passages (P3–P5) compared to the infant ADSCs (Fig. 2A). The expression of the *p53* gene in the infant ADSCs was higher than that in the UCSCs, but the difference was not significant. SA-β-gal staining at passage 7 showed more positive staining in the UCSCs than in the infant ADSCs (Fig. 2B). Additionally, immunofluorescence staining of γH2AX in the nuclei of the infant ADSCs and UCSCs showed that there were fewer fluorescent signals in the infant ADSCs than in the UCSCs (Fig. 2C, D). Furthermore, the levels of the SODs were measured. The expression levels of *SOD1* (a 2.81- ± 0.01-fold increase) (Fig. 3A), *SOD2* (a 9.44- ± 0.19-fold increase) (Fig. 3B), and *SOD3* (a 166- ± 0.04-fold increase) (Fig. 3C) were all significantly higher in the infant ADSCs than in the UCSCs. These results suggest that infant ADSCs have better anti-oxidative ability than the UCSCs.

3.3. Chondrogenic differentiation in the infant ADSCs and UCSCs

Chondrogenic differentiation was observed in both infant ADSCs and UCSCs, but the infant ADSCs were found to differentiate larger chondrogenic pellets compared to the UCSCs (Fig. 4A). The mean diameters of the differentiated pellets from the infant ADSCs were about 0.2 cm (0.2 ± 0.06 cm), which was significantly larger than the UCSC-differentiated pellets, with a mean diameter of about 0.15 cm (0.14 ± 0.03 cm) (Fig. 4B). The SOX9 gene expression, an early marker of chondrogenic differentiation, in the chondrogenic pellets differentiated from infant ADSCs on day 7, showed a 32.66- ± 17.55-fold increase compared to the control group. This increase was similar to the pellets formed from the UCSCs (a 31.83- ± 18.59-fold increase) (Fig. 4C). Late markers, such as collagen type 2 (*COL2*) and collagen type 10 (*COL10*) expression, had significantly higher fold increase in the infant ADSC-differentiated chondrogenic pellets (an 1825- ± 1026-fold increase and a 3565.2- ± 1451-fold increase, respectively) compared to those formed from the UCSCs (a 91.7- ± 61.25-fold increase and a 51.13- ± 22.35-fold increase, respectively) (Fig. 4D, E). The contents of glycosaminoglycans (GAGs) of infant ADSC- and UCSC-differentiated pellets were stained by Alcian blue, and the fold changes of the expression of the COL2 and COL10 protein were analyzed by immunohistochemistry staining (Fig. 5A; Fig. S1, http://links.lww.com/JCMA/A210). The intensities of the blue color of the infant ADSC-generated chondrogenic pellets stained by Alcian blue were similar to those of the UCSCs (Fig. 5B). The measured intensities of the UCSCs-generated pellets were set as the

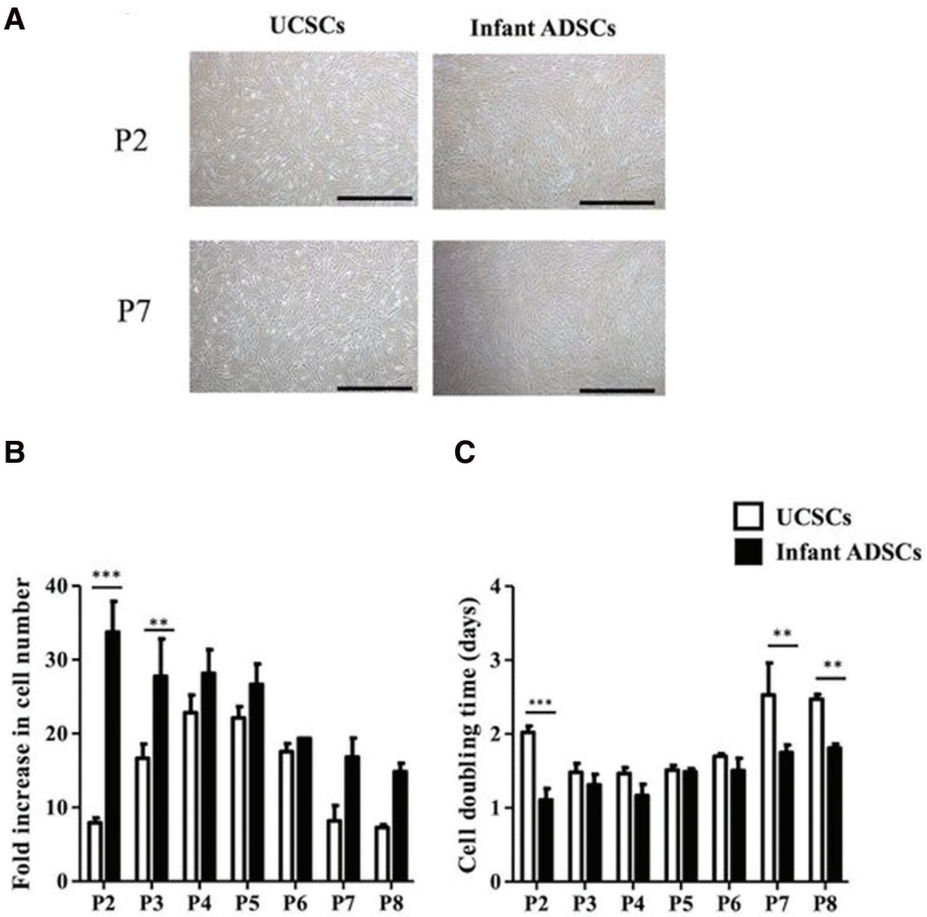

Fig. 1 Proliferation of the UCSCs and infant ADSCs. A, The morphology of UCSCs and infant ADSCs at passages 2 and 7 was observed using a phase contrast microscope (Nikon eclipse TS100) with a magnification of ×40. The scale bar represents 100 μm (B) the fold increases in cell numbers and (C) doubling time periods of UCSCs and infant ADSCs were calculated and compared from passages 2 (P2) to 8 (P8). The mean ± SEM with multiple experimental replicates is shown. The statistical significance of comparison between UCSCs and infant ADSCs was determined by the Mann-Whitney *U* test analysis. The symbol "**" indicates $p < 0.01$, and the symbol "***" indicates $p < 0.001$. ADSCs = adipose-derived mesenchymal stem cells; UCSCs = umbilical cord-derived mesenchymal stem cells.

standard to calculate the fold changes of the infant ADSC-generated pellets (a 1.04- ± 0.11-fold increase). Both the fold changes of the expression of COL2 and COL10 in the pellets formed from the infant ADSCs (a 1.78- ± 0.22-fold increase and a 1.41- ± 0.11-fold increase, respectively) were significantly higher than those formed from the UCSCs (Fig. 5C, D).

3.4. Osteogenic differentiation in the infant ADSCs and UCSCs

To assess the osteogenic differentiation of infant ADSCs and UCSCs, the fold changes in the expression of the osteocyte-related gene were measured after 21 days of differentiation. The relative expression fold changes of two important genes, runt-related transcription factor 2 (*RUNX2*) (Fig. 6A) and alkaline phosphatase (*ALP*) (Fig. 6B), were significantly higher in the infant ADSC-differentiated osteogenic cells, with a 5.52- ± 0.59-fold increase and a 45.06- ± 14.14-fold increase, respectively, compared to UCSC-differentiated cells, which showed only a 1.33- ± 0.25-fold increase and a 10.3- ± 2.77-fold increase, respectively. The calcium deposits in the infant ADSC- and UCSC-differentiated osteogenic cells on day 21 were stained by ARS to determine the degrees of osteogenic differentiation (Fig. 6C). Calcium deposits in the differentiated cells stained with ARS to determine the degree of osteogenic differentiation (Fig. 6C), and the intensity of staining was measured. The differentiated cells showed obvious red color compared to the undifferentiated cells (Fig. 6C; Fig. S2, http://links.lww.com/JCMA/A210). The intensity of ARS staining in infant ADSC-differentiated cells (a 32.14- ± 0.74-fold increase) was significantly higher than that in UCSC-differentiated cells (a 2.3- ± 0.25-fold increase) (Fig. 6D).

3.5. Adipogenic differentiation in the infant ADSCs and UCSCs

Adipogenic differentiation was investigated in infant ADSCs and UCSCs by detecting the expression of peroxisome proliferator-activated receptor γ (*PPARγ*) (Fig. 7A) and lipoprotein lipase (*LPL*) (Fig. 7B) genes on day 21. The fold changes in the expression levels of both genes were higher in the infant ADSC-differentiated adipogenic cells (a 48.8- ± 18.84-fold increase and a 70.82- ± 11.57-fold increase, respectively) than in the UCSC-differentiated cells (a 29.03- ± 6.74-fold increase and a 7.82- ± 2.12-fold increase, respectively), but the difference in *PPARγ* expression was not significant. Oil Red O staining of the lipids

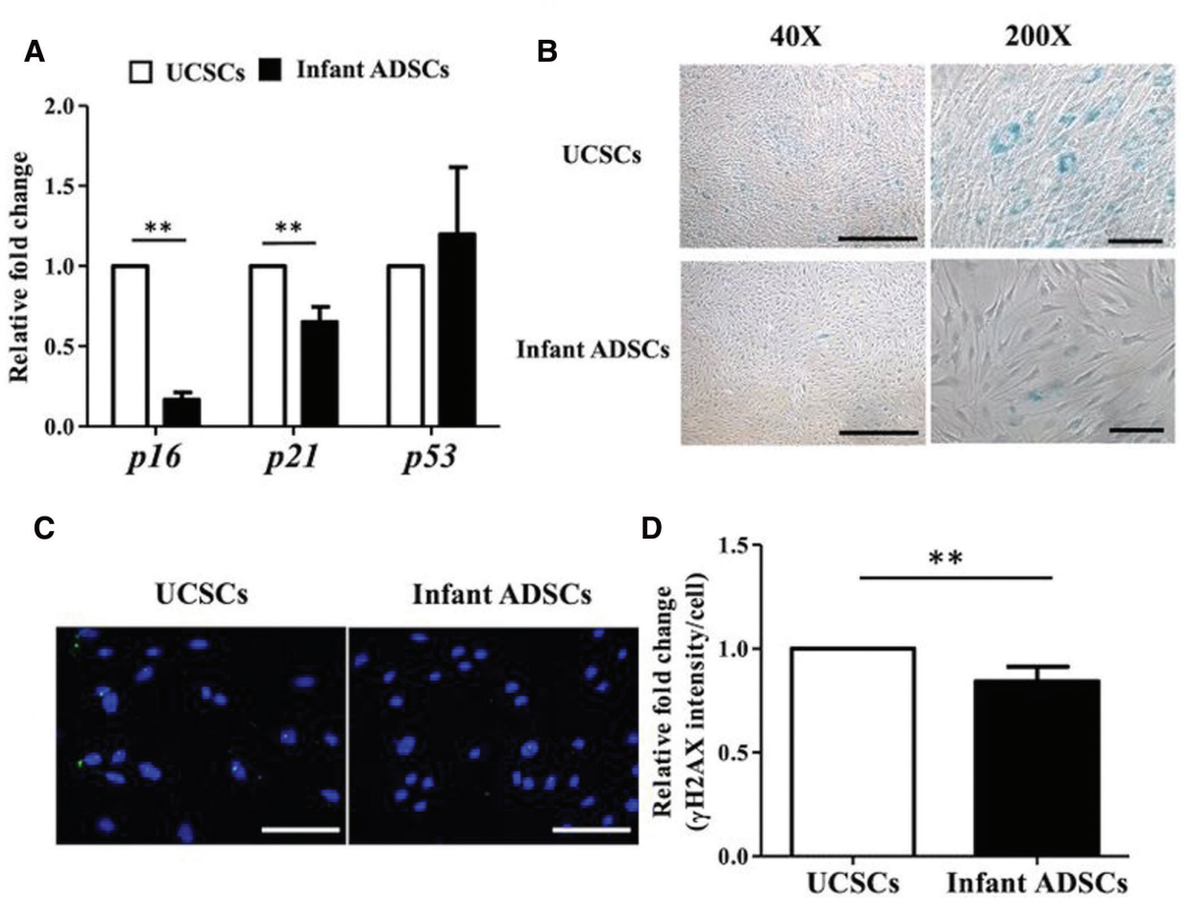

Fig. 2 Senescence and replicative stress in UCSCs and infant ADSCs. A, RT-qPCR analysis of senescence related-genes, including *P16*, *P21*, and *P53*, in UCSCs and infant ADSCs at passages 3–5. The values were normalized to the expression of *GAPDH*, and the relative fold changes were compared to UCSCs. Statistical significance of comparing UCSCs and infant ADSCs was determined by the Mann-Whitney *U* test. B, SA-β-gal staining of UCSCs and infant ADSCs and UCSCs at passage 7 was detected by a Senescence Detection Kit using a Nikon eclipse TS100 microscope. Blue-stained cells indicate positive SA-β-gal staining. Positive was stained and exhibited in blue. The left panel showed the cell image at ×40 magnification (the scale bar = 100 μm), and the right panel showed the cell image at ×200 magnification (the scale bar = 100 μm). C, Immunostaining of γH2AX (green) and DAPI (blue) in UCSCs and infant ADSCs at passage 3, detected by an Olympus BX43 microscope (magnification ×400, the scale bar = 100 μm). D, Quantification of γH2AX immunofluorescence intensity in the nuclei in the UCSCs and infant ADSCs. Values, which quantified by the Image-Pro Plus v4.5.0.29, were normalized to the cell numbers and compared to show the relative fold changes. Mean ± SEM with three replicates were expressed. Statistical significance of comparing infant ADSCs and UCSCs was determined by the Mann-Whitney *U* test. "**" represented $p < 0.01$. ADSCs = adipose-derived mesenchymal stem cells; DAPI = 4′,6-diamidino-2-phenylindole; *GAPDH* = glyceraldehyde-3-phosphate dehydrogenase; RT-qPCR = reverse transcription-quantitative polymerase chain reaction; SA-β-gal = senescence-associated β-galactosidase; UCSCs = umbilical cord-derived mesenchymal stem cells; γH2AX = phosphorylated histone variant H2AX.

in the adipogenic cells that differentiated from the infant ADSCs and UCSCs on day 21 shows red color compared to undifferentiated cells (Fig. 7C; Fig. S3, http://links.lww.com/JCMA/A210). The intensity of the Oil Red O staining was significantly higher in the infant ADSC-differentiated cells (a 5.27- ± 0.21-fold increase) than in the UCSC-differentiated cells (a 1.3- ± 0.10-fold increase) (Fig. 7D).

3.6. Hepatogenic differentiation in the infant ADSCs and UCSCs

The expression levels of albumin (*ALB*) and tyrosine aminotransferase (*TAT*), which are markers for hepatogenic differentiation, were measured in the infant ADSC-differentiated and UCSC-differentiated cells. The results showed that the fold changes in *ALB* expression (Fig. 8A) and *TAT* expression (Fig. 8B) were significantly higher in infant ADSCs (a 7.97- ± 1.35-fold increase and a 3.53- ± 0.23-fold increase, respectively) compared to UCSC (a 3.48- ± 0.94-fold increase and a 1.69- ± 0.49-fold increase, respectively). To further confirm these finding, albumin expression was detected using immunofluorescence staining (Fig. 8C; Fig. S4, http://links.lww.com/JCMA/A210). The quantified albumin expression in infant ADSC-differentiated hepatogenic cells (a 9.18- ± 1.06-fold increase) was significantly higher than that in UCSC-differentiated ones (a 2.72- ± 0.54-fold increase) (Fig. 8D).

3.7. Tenogenic differentiation in the infant ADSCs and UCSCs

The expression levels of the tendon-related genes, including matrix metallopeptidase 3 (*MMP3*) (Fig. 9A), decorin (*DCN*) (Fig. 9B), and collagen type 3 (*COL3*) (Fig. 9C), were compared in infant ADSCs and UCSCs after 21 days of tenogenic differentiation induction. The results showed that all of the fold changes in gene expression were significantly higher in

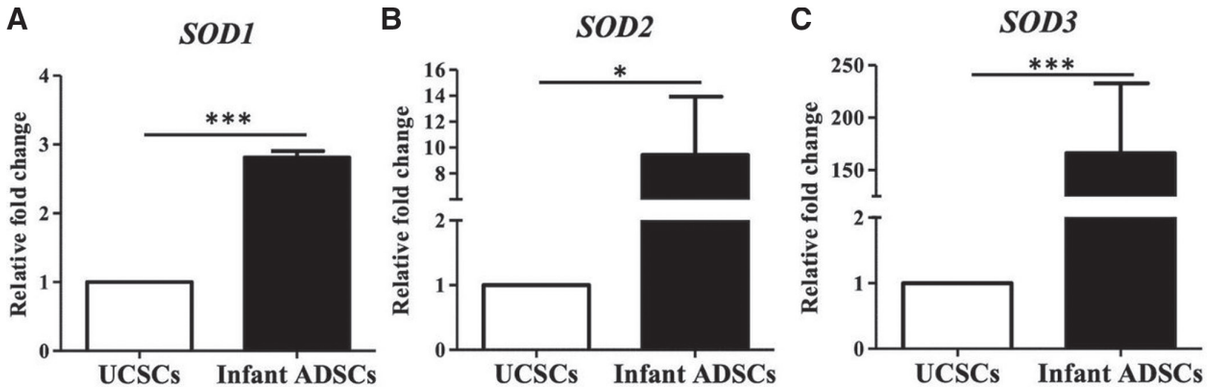

Fig. 3 *SOD* expression levels in UCSCs and infant ADSCs. A, The *SOD1*, (B) *SOD2*, and (C) *SOD3* genes of the UCSCs and infant ADSCs were detected by RT-qPCR, and the values were normalized to the expression of *GAPDH*. The value of the UCSCs was used as the standard to compare with that of the infant ADSCs, and the relative fold changes were shown. Mean ± SEM with three experimental replicates were expressed. Statistical significance of comparing the infant ADSCs and UCSCs was determined by the Mann-Whitney *U* test. "*" represented $p < 0.05$. "****" represented $p < 0.001$. ADSCs = adipose-derived mesenchymal stem cells; *GAPDH* = glyceraldehyde-3-phosphate dehydrogenase; RT-qPCR = reverse transcription-quantitative polymerase chain reaction; *SOD* = superoxide dismutase; UCSCs = umbilical cord-derived mesenchymal stem cells.

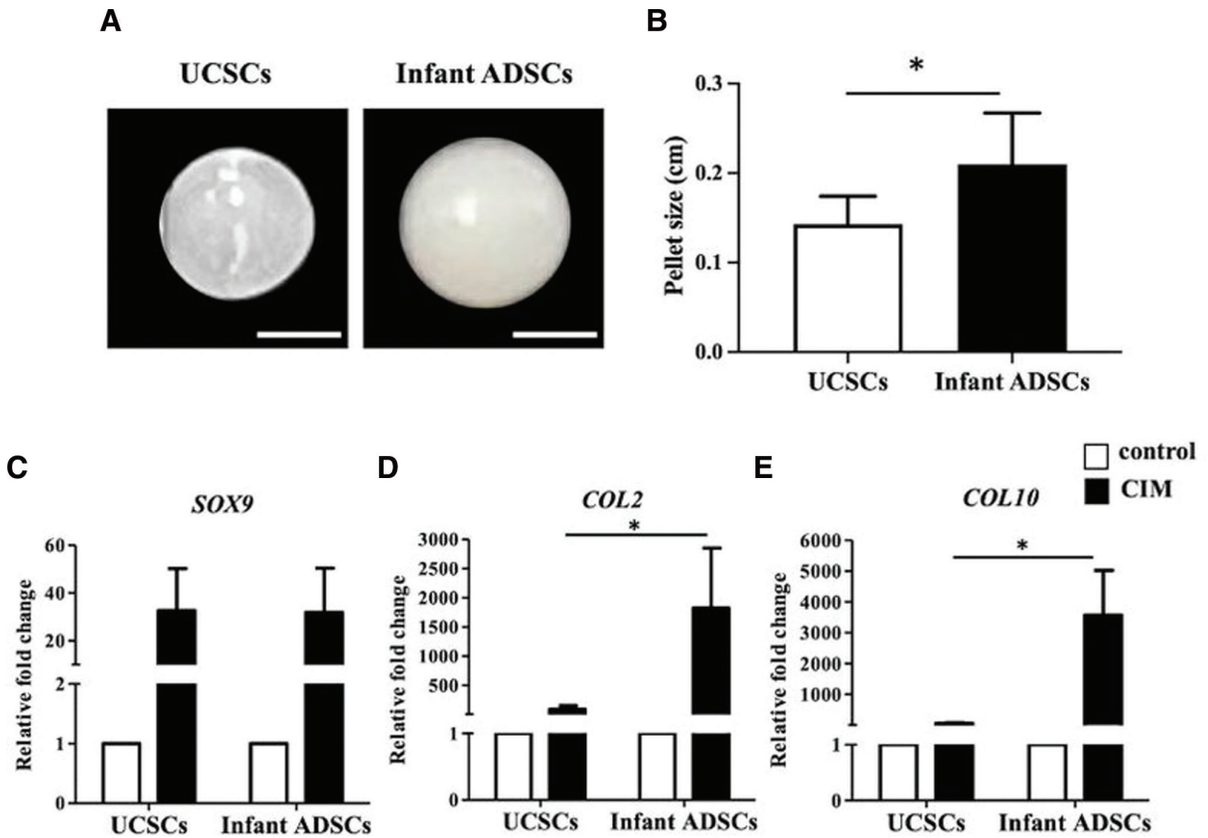

Fig. 4 In vitro chondrogenic differentiation of UCSCs and infant ADSCs. A, The chondrogenic pellets differentiated from passages 3 to 5 of the UCSCs and infant ADSCs (3×10^5 cells/pellet) on day 21 (the scale bar = 1 mm). B, The diameters of the pellets was measured on day 21. The expression levels of (C) *SOX9* on day 7, (D) *COL2*, and (E) *COL10* on day 21 of the UCSC- and infant ADSC-differentiated pellets were detected by RT-qPCR. The values were normalized to the expression of *GAPDH*. The gene expression of the undifferentiated cells was used as the standard to compare with that of the UCSC- and infant ADSC-differentiated chondrocyte-like cells, and the relative fold changes were shown. Mean ± SEM with three experimental replicates were expressed. Statistical significance of comparing the infant ADSCs- and UCSCs-differentiated pellets was determined by the Mann-Whitney *U* test. "*" represented $p < 0.05$. ADSCs = adipose-derived mesenchymal stem cells; CIM = chondrogenic differentiation medium; *COL* = collagen; *GAPDH* = glyceraldehyde-3-phosphate dehydrogenase; RT-qPCR = reverse transcription-quantitative polymerase chain reaction; *SOX9* = SRY-box containing gene 9; UCSCs = umbilical cord-derived mesenchymal stem cells.

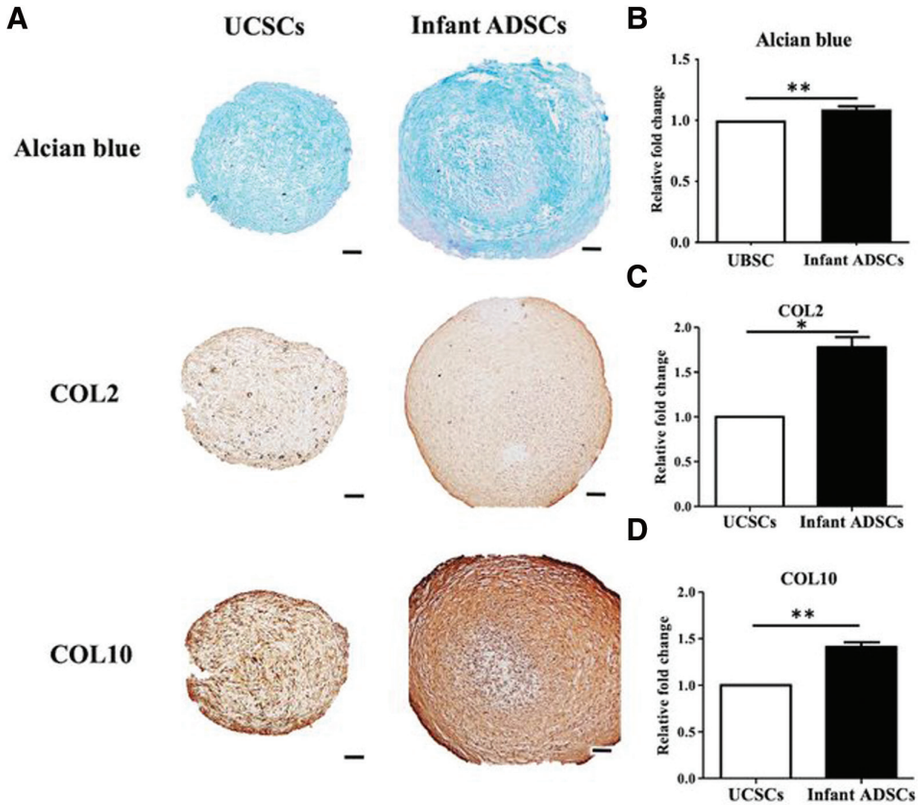

Fig. 5 Immunohistochemistry staining of UCSC- and infant ADSC-differentiated pellets. A, The pellets of the 21-d chondrogenic differentiated UCSCs and infant ADSCs were sectioned and stained with Alcian blue, anti-COL2, and anti-COL10 antibodies to detect the protein expression levels by immunostaining and evaluated by an Olympus BX43 microscope (magnification ×100, the scale bar = 200 μm). B–D, The intensities of each staining were measured and normalized with the whole backgrounds of the sections. The value of the UCSCs was used as the standard to compare with that of the infant ADSCs, and the relative fold changes were shown. Mean ± SEM with three experimental replicates were expressed. Statistical significance of comparing the UCSC- and infant ADSC-differentiated pellets was determined by the Mann-Whitney *U* test. "*" represented $p < 0.05$. "**" represented $p < 0.01$. ADSCs = adipose-derived mesenchymal stem cells; COL2 = collagen type 2; COL10 = collagen type 10; UCSCs = umbilical cord-derived mesenchymal stem cells.

UCSC-differentiated tenogenic cells (a 229.32- ± 76.96-fold increase, a 103- ± 34.01-fold increase, and a 2.98- ± 0.56-fold increase, respectively) compared to infant ADSCs (a 30.59- ± 16.10-fold increase, a 4.34- ± 0.86-fold increase, and a 1.61- ± 0.31-fold increase, respectively). To further confirm these finding, collagens in the 21-day differentiated tenogenic cells from infant ADSCs and UCSCs were stained with picrosirius red, which appeared in red (Fig. 9D; Fig. S5, http://links.lww.com/JCMA/A210). The picrosirius red staining was dissolved in a 0.2 M NaOH and methanol buffer, and the absorbance was measured by an ELISA reader. The results showed that the measured fold changes in UCSCs (a 1.59- ± 0.10-fold increase) were significantly higher than those in infant ADSCs (a 1.31- ± 0.05-fold increase) (Fig. 9E). Overall, compared to infant ADSCs, UCSCs showed a stronger tendency to differentiate into the tenogenic lineage, as evidenced by higher expression levels of tendon-related genes and collagen.

4. DISCUSSION

In our previous study, we conducted a comprehensive comparison of the properties of the infant ADSCs and adult ADSCs, including proliferation, anti-aging ability, antioxidation ability, and differentiation potential.[18] Our results demonstrated that infant ADSCs exhibited higher preservation of proliferation abilities, anti-senescence abilities, and antioxidation activities when compared to UCSCs. Furthermore, we found that infant ADSCs had a greater potential for differentiation toward chondrogenic, osteogenic, adipogenic, and hepatogenic lineages, while UCSCs showed a preference for tenogenic differentiation.

The low isolation efficiency and limited replicative lifespan of UCSCs have been reported in previous studies, which may limit their potential applications in tissue engineering.[25–27] In this study, we used UCSC cell lines purchased from the ATCC, which had limited passages and exhibited severe decline in proliferation at late passages. In contrast, the infant ADSCs showed higher preservation of proliferation abilities and could be preserved for longer periods of time. Moreover, our results are consistent with previous studies demonstrating that ADSCs collected from the infant patients with liver disease have more biological advantages compared to those collected from adults.[28] We collected infant ADSCs from the polydactyly fat tissue without other organic diseases, which further supports the potential use of these cells for tissue engineering applications. Overall, our finding suggests that infant ADSCs may be a more attractive material for tissue engineering compared to UCSCs.

Cellular senescence is a critical factor that influences the multilineage differentiation of MSCs.[29] In this study, we found that the senescence-related gene expression levels, including *p16*, *p21*, and *p53*, were higher in the UCSC cells at passages 3–5 compared to infant ADSCs. Moreover, UCSCs at passage 7 exhibited higher expression of SA-β-gal than infant ADSCs. Although UCSCs are collected from umbilical cord, which is the

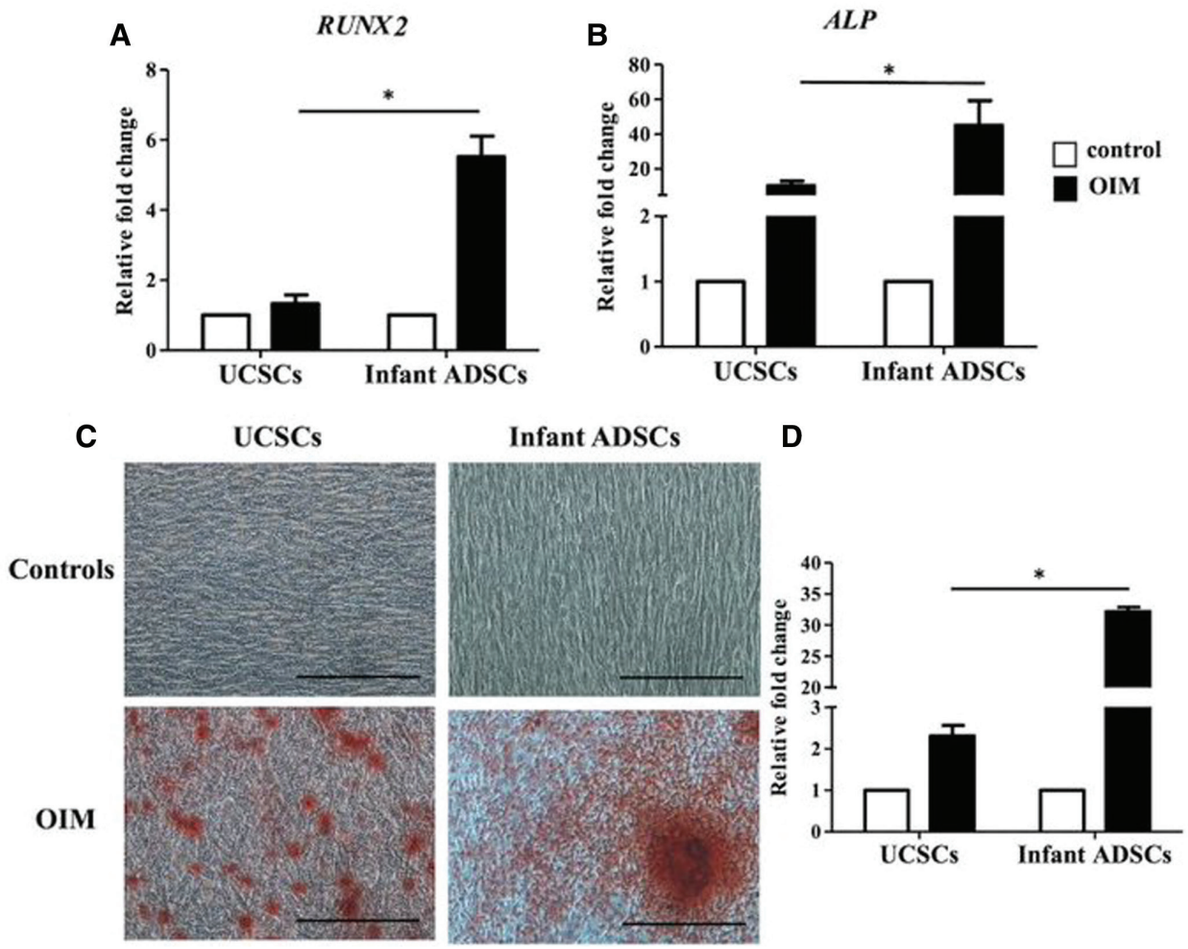

Fig. 6 In vitro osteogenic differentiation of UCSCs and infant ADSCs. Osteocyte-related genes, including the *RUNX2* (A) and *ALP* (B) of the UCSCs and infant ADSCs after having been treated with the factor-induced medium (OIM) for 21 d, were detected by RT-qPCR. The expression value of each gene was normalized to the expression of *GAPDH*. The gene expression of the undifferentiated cells was used as the standard to compare with that of the UCSC- and infant ADSC-differentiated osteocyte-like cells, and the relative fold changes were shown. C, The undifferentiated UCSCs and infant ADSCs used as the controls were stained with ARS. The 21-d osteogenic differentiated UCSCs and infant ADSCs were confirmed with the ARS staining and detected by a Nikon eclipse TS100 microscope (magnification ×200, the scale bar = 25 μm). D, The ARS staining were extracted from the stained cells and measured the OD at wavelength of 550 nm. The OD of differentiated cells was normalized with that of controls and the relative fold changes were shown. Mean ± SEM with three experimental replicates were expressed. Statistical significance of comparing the UCSC- and infant ADSC-differentiated osteogenic cells was determined by the Mann-Whitney *U* test. "*" represented $p < 0.05$. ADSCs = adipose-derived mesenchymal stem cells; *ALP* = alkaline phosphatase; ARS = Alizarin Red S; *GAPDH* = glyceraldehyde-3-phosphate dehydrogenase; OD = optical density; OIM = osteogenic induction medium; RT-qPCR = reverse transcription-quantitative polymerase chain reaction; *RUNX2* = runt-related transcription factor 2; UCSCs = umbilical cord-derived mesenchymal stem cells.

primary sample from neonates, our study showed that they were prone to senescence. This is consistent with a previous study that compared senescence in dental pulp-derived MSCs (DPSCs) and UCSCs at passage 6 and found significantly higher SA-β-gal expression in UCSCs.[30] Interestingly, despite UCSCs being assumed to be the youngest MSCs, our study showed that the ability of infant ADSCs to delay senescence was stronger than that of UCSCs.

ROS has been shown to potentially increase the stemness of ADSCs[31] and promote cell proliferation after exiting quiescence.[32] However, excessive ROS can have detrimental effects on MSCs and even lead to cell death.[33] Antioxidant enzymes play a critical role in counteracting the harmful effect of ROS.[34] SOD1 and SOD2 have been reported to enhance the therapeutic potential of ADSCs.[35,36] Previous studies, including this research study, have demonstrated that infant ADSCs exhibit higher expression of SOD genes than adult ADSCs[18] and UCSCs.

Age and senescence can have an impact on the differentiation potential of MSCs. In previous study, infant ADSCs demonstrated better differentiation potential toward chondrogenesis, adipogenesis, and neurogenesis but showed less osteogenic and tenogenic tendencies compared to adult ADSCs.[18] While ADSCs and UCSCs share similar morphologies and immunophenotypes, their differentiation tendencies are diverse. Cytochemistry analysis showed that osteogenic and chondrogenic differentiation of BMSCs, ADSCs, and UCSCs were similar. However, UCSCs exhibited restricted or delayed adipogenic differentiation with fewer and smaller lipid vacuoles.[25,27] The differentiation of MSCs toward specific lineage is associated with the intrinsic mechanical properties such as elasticity and viscosity.[37] UCSCs were found to have higher cell stiffness compared to BMSCs and ADSCs, with ADSCs exhibiting the lowest stiffness. UCSCs prefer osteogenic differentiation due to

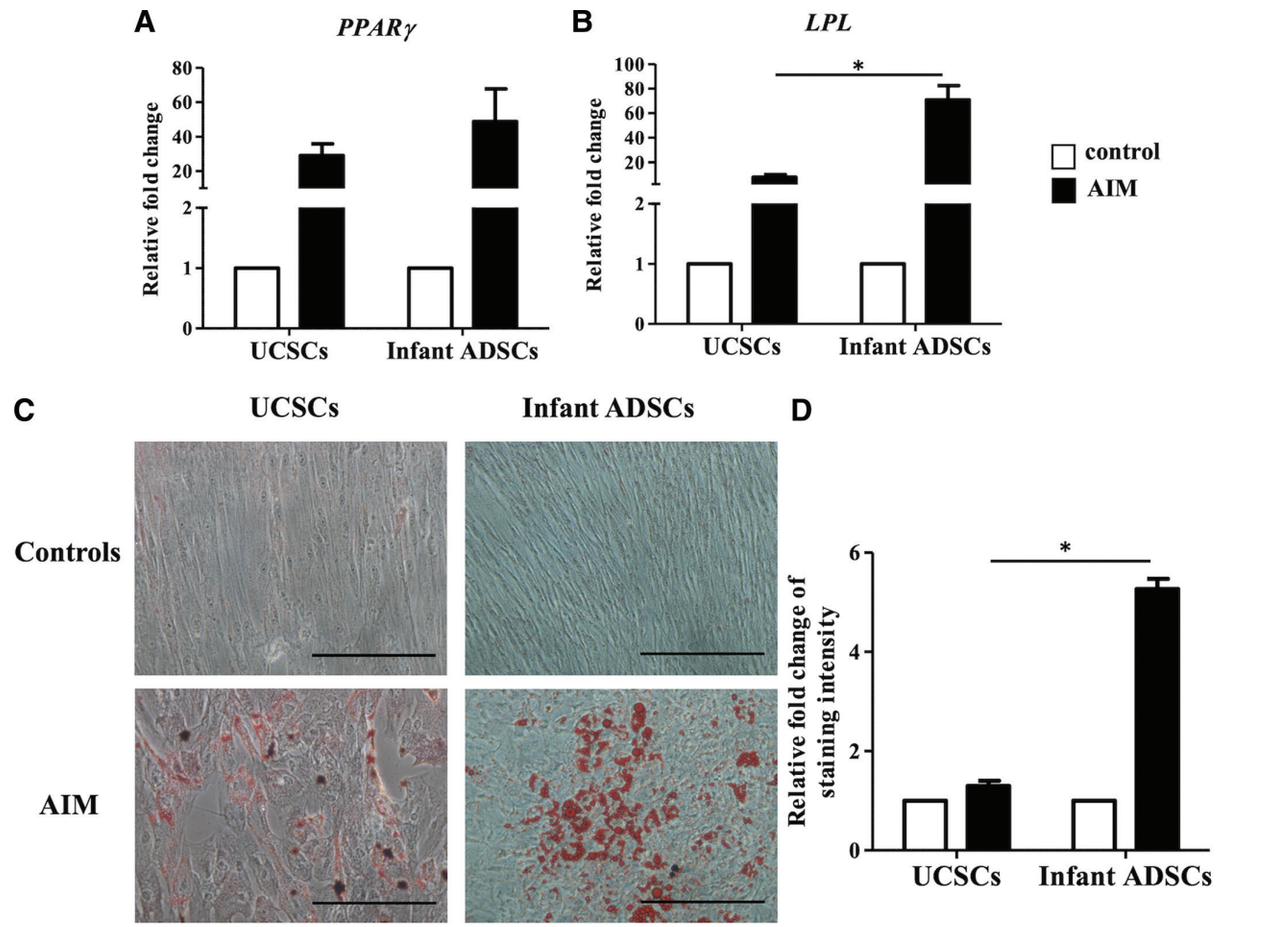

Fig. 7 In vitro adipogenic differentiation of UCSCs and infant ADSCs. Adipose-related genes, including *PPARγ* (A) and *LPL* (B) of the UCSCs and infant ADSCs after having been treated with the factor-induced medium (AIM) for 21 d, were detected by RT-qPCR. The expression value of each gene was normalized to the expression of *GAPDH*. The gene expression of the undifferentiated cells was used as the standard to compare with that of the UCSC- and infant ADSC-differentiated adipocyte-like cells, and the relative fold changes were shown. C, The undifferentiated UCSCs and infant ADSCs used as the controls were stained with Oil Red O. The 21-d adipogenic differentiated UCSCs and infant ADSCs were confirmed with the Oil Red O staining and detected by a Nikon eclipse TS100 microscope (magnification ×200, the scale bar = 25 μm). D, The Oil Red O staining were extracted from the stained cells and measured the OD at wavelength of 510 nm. The OD of differentiated cells was normalized with that of undifferentiated cells and the relative fold changes were shown. Mean ± SEM with three experimental replicates were expressed. Statistical significance of comparing the UCSC- and infant ADSC-differentiated adipogenic cells was determined by the Mann-Whitney *U* test. "*" represented $p < 0.05$. ADSCs = adipose-derived mesenchymal stem cells; AIM = adipogenic induction medium; *GAPDH* = glyceraldehyde-3-phosphate dehydrogenase; *LPL* = lipoprotein lipase; OD = optical density; *PPARγ* = peroxisome proliferator-activated receptor-γ; RT-qPCR = reverse transcription-quantitative polymerase chain reaction; UCSCs = umbilical cord-derived mesenchymal stem cells.

their high stiffness, whereas ADSCs showed a preference for adipogenic differentiation.[8] However, in this study, infant ADSCs showed better chondrogenic, osteogenic, adipogenic, and hepatogenic differentiation potential than UCSCs, while only the tenogenic differentiation of the UCSCs was enhanced. These finding suggest the differentiation potential of infant ADSCs is more diverse.

In this study, the lack of time course detection of differentiated gene expression levels may have overlooked the possibility of delayed differentiation in the UCSCs. For example, previous research has demonstrated that the adipogenic differentiation of UCSCs required more time to occur.[4] In addition, inconsistencies in the effects of differentiation induction media on infant ADSCs and UCSCs could be a potential issue. Nevertheless, our study was designed to compare the differentiation potential of the infant ADSCs and UCSCs under the same condition.

Our results showed that infant ADSCs exhibited the highest proliferation abilities and retained more stemness, suggesting that excised polydactyly fat tissue could be an ideal source of ADSCs for tissue engineering application.

ACKNOWLEDGMENTS

This study was supported in part by grants from the Taipei Veterans General Hospital (V111C-231), the Ministry of Science and Technology (MOST 111-2314-B-075-057-MY3), the Taoyuan General Hospital, Ministry of Health and Welfare (PTH111067), and the Ditmanson Medical Foundation Chiayi Christian Hospital (R110-45).

We thank the work that was assisted in part by the Division of the Experimental Surgery of the Department of Surgery, Taipei Veterans General Hospital.

APPENDIX A. SUPPLEMENTARY DATA

Supplementary data related to this article can be found at http://links.lww.com/JCMA/A210.

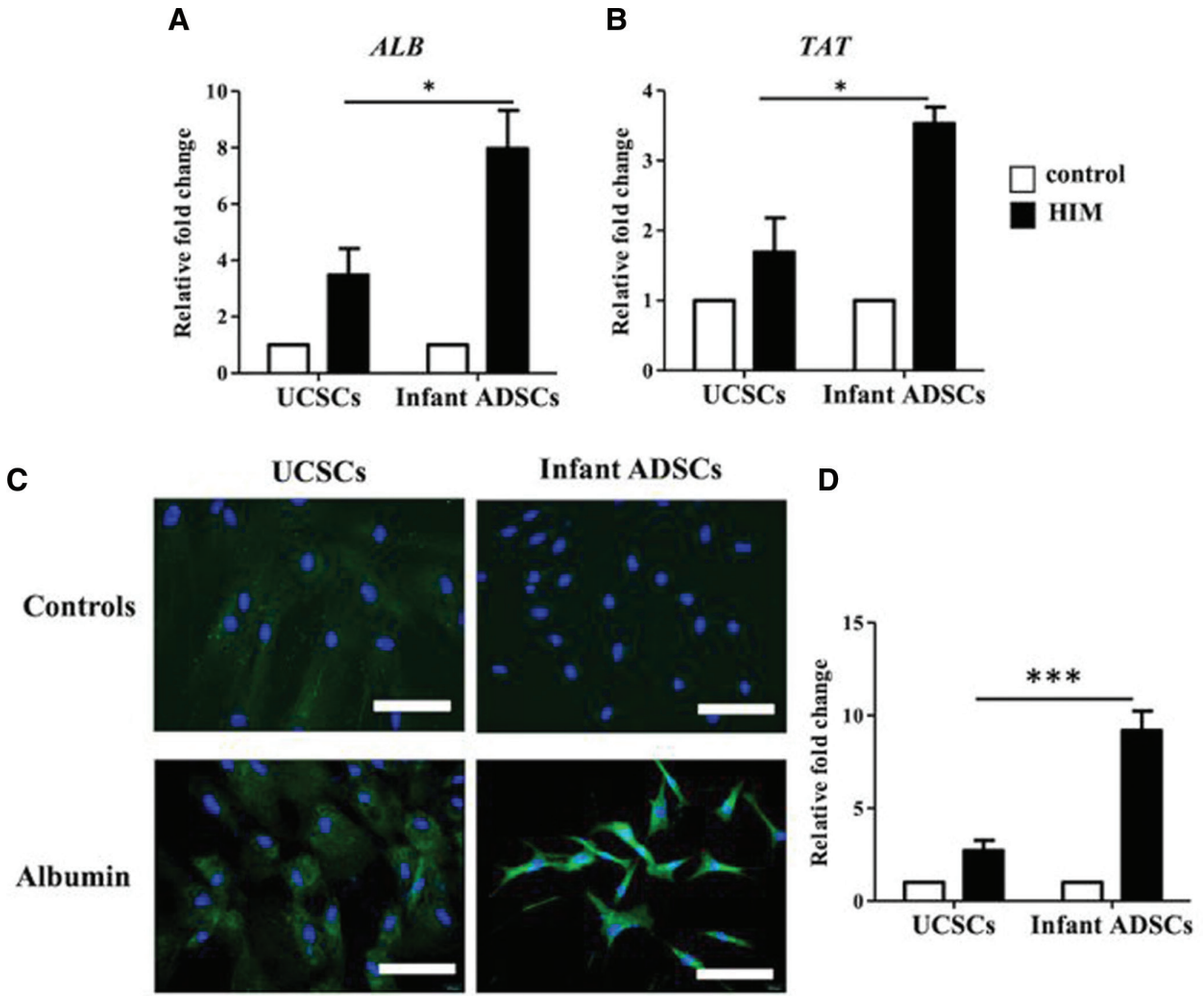

Fig. 8 In vitro hepatogenic differentiation of UCSCs and infant ADSCs. Hepatocyte-related genes, including matrix *ALB* (A) and *TAT* (B) of the UCSCs and infant ADSCs after having been treated with the HIM for 13–15 d, were detected by RT-qPCR. The expression value of each gene was normalized to the expression of *GAPDH*. The gene expression of the undifferentiated cells was used as the standard to compare with that of the UCSC- and infant ADSC-differentiated hepatocyte-like cells, and the relative fold changes were shown. C, The undifferentiated UCSCs and infant ADSCs used as the controls were stained with DAPI and antibodies. ALB protein in the UCSCs and infant ADSCs was detected by immunofluorescence staining shown in green fluorescence and evaluated with an Olympus BX43 microscope. The DNA stained by DAPI was shown in blue florescence (magnification ×400, the scale bar = 100 μm). D, The immunofluorescence intensity was quantified by the Image-Pro Plus v4.5.0.29. Mean ± SEM with three experimental replicates were expressed. Statistical significance of comparing the UCSC- and infant ADSC-differentiated neurogenic cells was determined by the Mann-Whitney *U* test. "*" represented $p < 0.05$. "***" represented $p < 0.001$. ADSCs = adipose-derived mesenchymal stem cells; *ALB* = albumin; DAPI = 4′,6-diamidino-2-phenylindole; *GAPDH* = glyceraldehyde-3-phosphate dehydrogenase; HIM = hepatogenic-induced medium; RT-qPCR = reverse transcription-quantitative polymerase chain reaction; *TAT* = tyrosine aminotransferase; UCSCs = umbilical cord-derived mesenchymal stem cells.

REFERENCES

1. Pittenger MF, Mackay AM, Beck SC, Jaiswal RK, Douglas R, Mosca JD, et al. Multilineage potential of adult human mesenchymal stem cells. *Science* 1999;284:143–7.
2. Kern S, Eichler H, Stoeve J, Klüter H, Bieback K. Comparative analysis of mesenchymal stem cells from bone marrow, umbilical cord blood, or adipose tissue. *Stem Cells* 2006;24:1294–301.
3. Zuk PA, Zhu M, Ashjian P, De Ugarte DA, Huang JI, Mizuno H, et al. Human adipose tissue is a source of multipotent stem cells. *Mol Biol Cell* 2002;13:4279–95.
4. Karahuseyinoglu S, Cinar O, Kilic E, Kara F, Akay GG, Demiralp DO, et al. Biology of stem cells in human umbilical cord stroma: in situ and in vitro surveys. *Stem Cells* 2007;25:319–31.
5. Rubinstein P, Rosenfield RE, Adamson JW, Stevens CE. Stored placental blood for unrelated bone marrow reconstitution. *Blood* 1993;81:1679–90.
6. Nanaev AK, Kohnen G, Milovanov AP, Domogatsky SP, Kaufmann P. Stromal differentiation and architecture of the human umbilical cord. *Placenta* 1997;18:53–64.
7. Fong CY, Richards M, Manasi N, Biswas A, Bongso A. Comparative growth behaviour and characterization of stem cells from human Wharton's jelly. *Reprod Biomed Online* 2007;15:708–18.
8. Han I, Kwon BS, Park HK, Kim KS. Differentiation potential of mesenchymal stem cells is related to their intrinsic mechanical properties. *Int Neurourol J* 2017;21(Suppl 1):S24–31.
9. Lasry A, Ben-Neriah Y. Senescence-associated inflammatory responses: aging and cancer perspectives. *Trends Immunol* 2015;36:217–28.
10. Zhang Y, Ravikumar M, Ling L, Nurcombe V, Cool SM. Age-related changes in the inflammatory status of human mesenchymal stem cells: implications for cell therapy. *Stem Cell Rep* 2021;16:694–707.
11. Alraies A, Alaidaroos NY, Waddington RJ, Moseley R, Sloan AJ. Variation in human dental pulp stem cell ageing profiles reflect contrasting proliferative and regenerative capabilities. *BMC Cell Biol* 2017;18:12.
12. Stolzing A, Jones E, McGonagle D, Scutt A. Age-related changes in human bone marrow-derived mesenchymal stem cells: consequences for cell therapies. *Mech Ageing Dev* 2008;129:163–73.

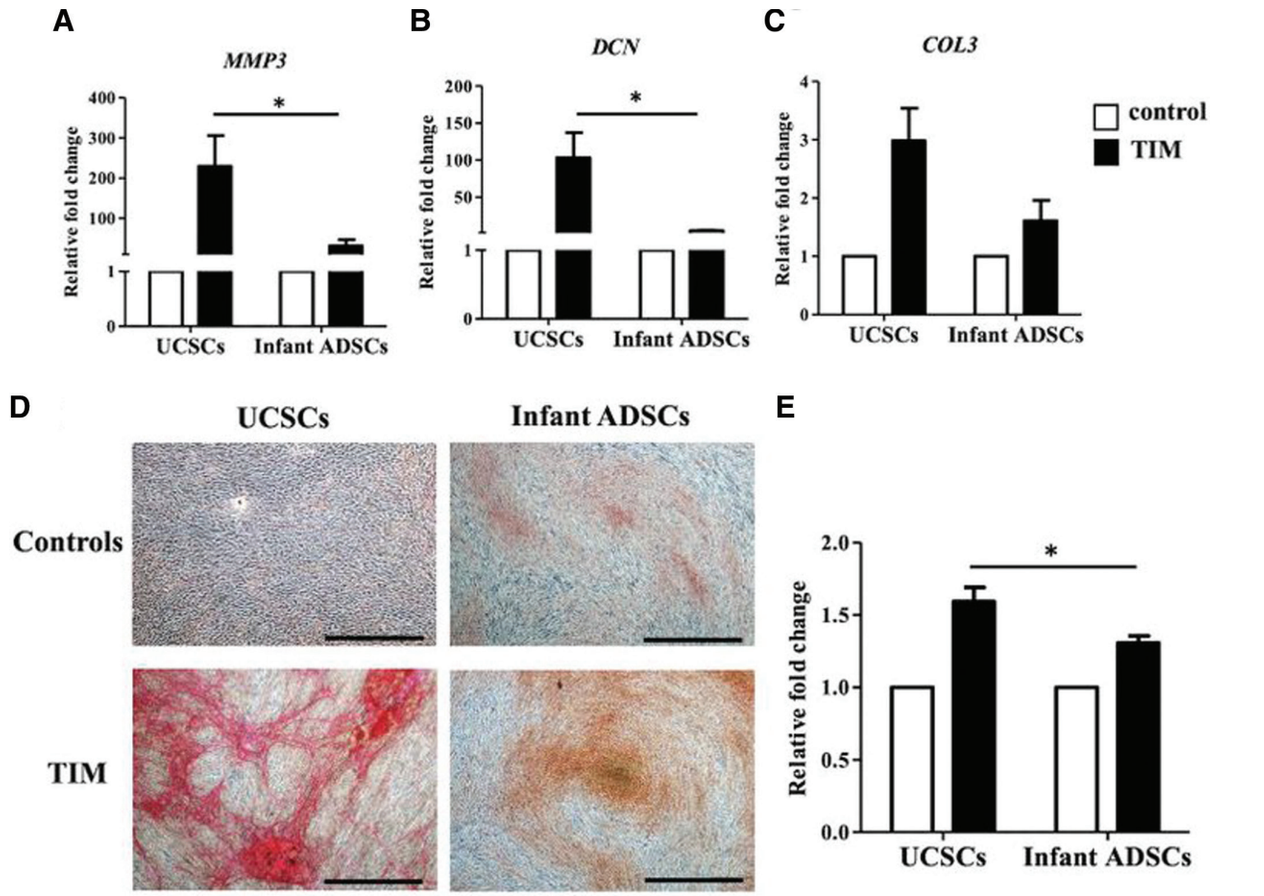

Fig. 9 In vitro tenogenic differentiation of UCSCs and infant ADSCs. Tendon-related genes, including *MMP3* (A), *DCN* (B), and *COL3* (C) of the UCSCs and infant ADSCs after having been treated with the TIM for 21 d, were detected by RT-qPCR. The expression value of each gene was normalized to the expression of *GAPDH*. The gene expression of the undifferentiated cells was used as the standard to compare with that of the UCSC- and infant ADSC-differentiated tendon-like cells, and the relative fold changes were shown. D, The undifferentiated UCSCs and infant ADSCs used as the controls were stained with picrosirius red. The 21-d tenogenic differentiated UCSCs and infant ADSCs were confirmed with the picrosirius red staining and detected by a Nikon eclipse TS100 microscope (magnification ×40, the scale bar = 100 μm). E, The intensities of the picrosirius red staining were measured by detecting the OD at wavelength of 550 nm and were normalized with that of controls and the relative fold changes were show. Mean ± SEM with three experimental replicates were expressed. Statistical significance of comparing the UCSC- and infant ADSC-differentiated tenogenic cells was determined by the Mann-Whitney *U* test. "*" represented $p < 0.05$. ADSCs = adipose-derived mesenchymal stem cells; *COL3* = collagen type 3; *DCN* = decorin; *GAPDH* = glyceraldehyde-3-phosphate dehydrogenase; *MMP3* = matrix metallopeptidase 3; OD = optical density; RT-qPCR = reverse transcription-quantitative polymerase chain reaction; TIM = tenogenic induction medium; UCSCs = umbilical cord-derived mesenchymal stem cells.

13. Choudhery MS, Badowski M, Muise A, Pierce J, Harris DT. Donor age negatively impacts adipose tissue-derived mesenchymal stem cell expansion and differentiation. *J Transl Med* 2014;12:8.
14. Neri S, Borzì RM. Molecular mechanisms contributing to mesenchymal stromal cell aging. *Biomolecules* 2020;10:340.
15. Castilla E, Paz J, Mutchinick O, Munoz E, Giorgiutti E, Gelman Z. Polydactyly: a genetic study in South America. *Am J Hum Genet* 1973;25:405–12.
16. Umair M, Ahmad F, Bilal M, Ahmad W, Alfadhel M. Clinical genetics of polydactyly: an updated review. *Front Genet* 2018;9:447.
17. Chen LJ, Chiou JY, Huang JY, Su PH, Chen JY. Birth defects in Taiwan: a 10-year nationwide population-based, cohort study. *J Formos Med Assoc* 2020;119:553–9.
18. Wu SH, Yu JH, Liao YT, Liu KH, Chiang ER, Chang MC, et al. Comparison of the infant and adult adipose-derived mesenchymal stem cells in proliferation, senescence, anti-oxidative ability and differentiation potential. *Tissue Eng Regen Med* 2022;19:589–601.
19. Buyl K, De Kock J, Najar M, Lagneaux L, Branson S, Rogiers V, et al. Characterization of hepatic markers in human Wharton's Jelly-derived mesenchymal stem cells. *Toxicol In Vitro* 2014;28:113–9.
20. Wang JP, Liao YT, Wu SH, Huang HK, Chou PH, Chiang ER. Adipose-derived mesenchymal stem cells from a hypoxic culture reduce cartilage damage. *Stem Cell Rev Rep* 2021;17:1796–809.
21. Hung SC, Chen NJ, Hsieh SL, Li H, Ma HL, Lo WH. Isolation and characterization of size-sieved stem cells from human bone marrow. *Stem Cells* 2002;20:249–58.
22. Wang JP, Hui YJ, Wang ST, Yu HH, Huang YC, Chiang ER, et al. Recapitulation of fibromatosis nodule by multipotential stem cells in immunodeficient mice. *PLoS One* 2011;6:e24050.
23. Stanco D, Caprara C, Ciardelli G, Mariotta L, Gola M, Minonzio G, et al. Tenogenic differentiation protocol in xenogenic-free media enhances tendon-related marker expression in ASCs. *PLoS One* 2019;14:e0212192.
24. Sweat F, Puchtler H, Rosenthal SI. Sirius red F3BA as a stain for connective tissue. *Arch Pathol* 1964;78:69–72.
25. Rebelatto CK, Aguiar AM, Moretão MP, Senegaglia AC, Hansen P, Barchiki F, et al. Dissimilar differentiation of mesenchymal stem cells from bone marrow, umbilical cord blood, and adipose tissue. *Exp Biol Med (Maywood)* 2008;233:901–13.
26. Wexler SA, Donaldson C, Denning-Kendall P, Rice C, Bradley B, Hows JM. Adult bone marrow is a rich source of human mesenchymal 'stem' cells but umbilical cord and mobilized adult blood are not. *Br J Haematol* 2003;121:368–74.
27. Rashnonejad A, Ercan G, Gunduz C, Akdemir A, Tiftikcioglu YO. Comparative analysis of human UCB and adipose tissue-derived

mesenchymal stem cells for their differentiation potential into brown and white adipocytes. *Mol Biol Rep* 2018;45:233–44.
28. Jin Y, Yang L, Zhang Y, Gao W, Yao Z, Song Y, et al. Effects of age on biological and functional characterization of adipose-derived stem cells from patients with end-stage liver disease. *Mol Med Rep* 2017;16:3510–8.
29. Drela K, Stanaszek L, Nowakowski A, Kuczynska Z, Lukomska B. Experimental strategies of mesenchymal stem cell propagation: adverse events and potential risk of functional changes. *Stem Cells Int* 2019;2019:7012692.
30. Das M, Das A, Barui A, Paul RR. Comparative evaluation of proliferative potential and replicative senescence associated changes in mesenchymal stem cells derived from dental pulp and umbilical cord. *Cell Tissue Bank* 2022;23:157–70.
31. Cheng NC, Hsieh TY, Lai HS, Young TH. High glucose-induced reactive oxygen species generation promotes stemness in human adipose-derived stem cells. *Cytotherapy* 2016;18:371–83.
32. Lyublinskaya OG, Borisov YG, Pugovkina NA, Smirnova IS, Obidina JV, Ivanova JS, et al. Reactive oxygen species are required for human mesenchymal stem cells to initiate proliferation after the quiescence exit. *Oxid Med Cell Longev* 2015;2015:502105.
33. Chang W, Song BW, Moon JY, Cha MJ, Ham O, Lee SY, et al. Anti-death strategies against oxidative stress in grafted mesenchymal stem cells. *Histol Histopathol* 2013;28:1529–36.
34. Chan PH. Reactive oxygen radicals in signaling and damage in the ischemic brain. *J Cereb Blood Flow Metab* 2001;21:2–14.
35. Yoo DY, Kim DW, Chung JY, Jung HY, Kim JW, Yoon YS, et al. Cu, Zn-superoxide dismutase increases the therapeutic potential of adipose-derived mesenchymal stem cells by maintaining antioxidant enzyme levels. *Neurochem Res* 2016;41:3300–7.
36. Sen S, Domingues CC, Rouphael C, Chou C, Kim C, Yadava N. Genetic modification of human mesenchymal stem cells helps to reduce adiposity and improve glucose tolerance in an obese diabetic mouse model. *Stem Cell Res Ther* 2015;6:242.
37. González-Cruz RD, Fonseca VC, Darling EM. Cellular mechanical properties reflect the differentiation potential of adipose-derived mesenchymal stem cells. *Proc Natl Acad Sci U S A* 2012;109:E1523–9.